Heliyon 10 (2024) e28386

Contents lists available at ScienceDirect

Heliyon

journal homepage: www.cell.com/heliyon

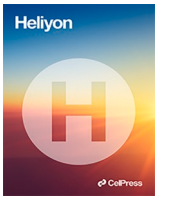

Research article

Qntrolling the LncRNA HULC-Tregs-PD-1 axis inhibits immune escape in the tumor microenvironment

XiaoYu Wang [a,1], Xiaoyan Mo [b,1], Zhuolin Yang [a], Changlin Zhao [a,b,*]

[a] School of Health Science, Guangdong Pharmaceutical University, Guangzhou, 51006, China
[b] The First Affiliated Hospital, Guangdong Pharmaceutical University, Guangzhou, 51006, China

ARTICLE INFO

Keywords:
Tumor microenvironment
lncRNA HULC
Tregs
PD-1
Immunotherapy

ABSTRACT

Background: Immune escape remains a major challenge in the treatment of malignant tumors. Here, we studied the mechanisms underlying immune escape in the tumor microenvironment and identified a potential therapeutic target.

Methods: Pathological specimens from patients with liver cancer, soft tissue sarcoma, and liver metastasis of colon cancer were subjected to immunohistochemistry analysis to detect the expression of programmed death-1 (PD-1) in the tumor microenvironment (TME). Additionally, the expression of regulatory T cells (Tregs) and long non-coding RNAs (lncRNAs), such as highly upregulated in liver cancer (HULC) was evaluated by fluorescence in situ hybridization, and the relationship between HULC, Treg cells, and PD-1 was determined. The animals were divided into H22 hepatic carcinoma and S180 sarcoma groups. Each group was divided into $^{Foxp3-/-}$C57BL/6J and C57BL/6J mice. Thereafter, mice were inoculated with 0.1 ml S180 sarcoma cells or 0.1 ml H22 hepatoma cells, at a concentration of 1×10^7/ml. The number of splenic $CD4^+CD25^+Foxp3^+$ T cells was detected by flow cytometry, and serum interleukin-10 (IL-10) and transforming growth factor β1 (TGF-β1) levels were detected using a Luminex liquid suspension chip. Expression of PD-1, fork head box P3 (*Foxp3*), and *HULC* in the TME, were analyzed and the therapeutic effect of inhibiting the lncRNA HULC-Treg-PD-1 axis in malignant tumors was determined.

Results: High expression of lncRNA HULC promotes the proliferation of Treg cells and increases PD-1 expression in the tumor microenvironment. The HULC-Treg-PD-1 axis plays an immunosuppressive role and promotes the proliferation of malignant tumors. Knocking out the *Foxp3* gene can affect the HULC-Treg-PD-1 axis and reduce PD-1, IL-10, and TGF-β1 expression to control the growth of malignant tumors.

Conclusion: The lncRNA HULC-Treg-PD-1 axis promotes the growth of malignant tumors. This axis could be modulated to reduce PD-1, IL-10, and TGF-β1 expression and the subsequent immune escape. The inhibition of immune escape in the tumor microenvironment can be achieved by controlling the LncRNA HULC-Treg-PD-1 axis.

* Corresponding author. School of Health Science, Guangdong Pharmaceutical University, Guangzhou, 51006, China.
E-mail address: zhaochanglin@gdpu.edu.cn (C. Zhao).
[1] Xiaoyu Wang and Xiaoyan Mo have contributed equally.

https://doi.org/10.1016/j.heliyon.2024.e28386
Received 6 December 2022; Received in revised form 15 March 2024; Accepted 18 March 2024
Available online 23 March 2024

1. Introduction

Programmed death-1 (PD-1)/programmed cell death ligand 1 (PD-L1) blockade therapy has become one of the most promising methods for tumor treatment. However, T cells exhaustion can affect the efficacy of the PD-1/PD-L1 blockade therapy [1]. Modulating immune activation and limiting immunopathology is a characteristic feature of regulatory T cells (Tregs) [2]. Treg cells inhibit inflammation; restrict the responses against autoantigens, symbiotic microorganisms, allergens, and pathogens; and regulate the homeostasis and functioning of the immune system [3,4]. The immune response regulates the physiological state of the body, and an imbalance in immune tolerance can lead to autoimmune diseases and persistent infections [5,6]. Hepatitis C virus (HCV) infection can inhibit the numbers and function of Tregs [7]. Treg cells play a key role in autoimmune liver disease and chronic viral hepatitis, and may be the key cell types targeted by immunotherapy during severe liver disease [8]. Within the tumor microenvironment (TME), Treg cells limit the anti-tumor immune response [9,10]. Forkhead box P3 (Foxp3) is a key transcription factor that controls the development and function of Tregs. $CD4^+CD25^+Foxp3^+$ T cells are identified as a Tregs and have been extensively studied in mammals, and produced large amounts of IL-10, TGF-β, CTLA-4, and CTLA-3 mRNA [11]. Treg cells in the spleens of mice and peripheral blood of humans are defined as $CD4^+CD25^+Foxp3^+$T cells and can be detected using flow cytometry antibodies.

Long non-coding RNAs (lncRNAs) affect the expression of genes at multiple levels through various mechanisms, such as by altering DNA methylation, histone modification, post-transcriptional regulation, RNA interference, and genetic imprinting, and participate in the initiation, growth, infiltration, metastasis, and recurrence of tumors. [12] The highly upregulated in liver cancer (*HULC*) gene is located on chromosome 6p24.3 and is 1.6 kb in length. It is the first lncRNA to be identified among the lncRNAs that are overexpressed in liver cancer [13]. The increase in HULC levels in liver cancer specimens and serum is dependent on the liver cancer grade and status of hepatitis B virus positivity [14]. Hepatitis B virus X protein (HBx) activates the HULC promoter through the cyclic adenosine monophosphate response element binding protein (CREB), which can promote the expression of HULC in liver cells, thereby inhibiting the expression of the tumor suppressor gene p18 and promoting the proliferation of liver cancer cells [15]. lncRNAs promote cancer metastasis [16,17]. The lncRNA HULC promotes the proliferation of liver cancer cells through CREB phosphorylation [18]. In case of the liver cancer caused by HBV, HBx downregulates tumor suppressor gene p18 to regulate the promoter region of HULC and increases HULC expression and tumor cell proliferation [19]. LncRNAs have important applications in the diagnosis, treatment, and prevention of hepatic carcinoma (HCC) [20]. In the TME, cancer cells overexpress PD-L1, which binds to PD-1 on cytotoxic T cells to suppress T cell activation and function [21]. Circulating Tregs and HULC were significantly upregulated in plasma samples of HBV associated cirrhosis patients, and overexpression of HULC in lentiviral vectors increase the frequency of Treg *in vitro* [22].

Here, we demonstrate that regulating the LncRNA HULC-Treg-PD-1 axis can facilitate a decrease in the expression of PD-1, interleukin-10 (IL-10), and transforming growth factor β1 (TGF-β1), and reduce immune escape in the TME.

2. Materials and methods

2.1. Patients and specimens

This study was a retrospective case analysis. The patients were divided into liver cancer (n = 30), colon cancer with liver metastasis (n = 30), and soft tissue sarcoma (n = 32) groups. The enrolled patients were not administered interventional therapy, targeted therapy, chemotherapy, or immunotherapy, excluding pulmonary infection and cholecystitis. Written informed consent was obtained from all patients. The study was approved by the ethics committee of Guangdong Clifford hospital, China (approval no. 2/2018-12).

Specimens were obtained following surgery or biopsy, collection was conducted from January 2018 to December 2021. Expression of IL-10, TGF-β1, and PD-1 proteins in the samples was detected using immunohistochemistry (IHC). Expression of *FOXP3* and lncRNA *HULC* was detected using fluorescence in situ hybridization (FISH). In liver cancer cases, the numbers of $CD4^+CD25^+Foxp3^+$T cells in the serum, as well as the concentrations of IL-10 and TGF-β1, with healthy people as a control, were analyzed.

2.2. Animal experiments

C57BL/6J mice were purchased from Guangdong Medical Experimental Animal Center, and Foxp3 knockout mice ($^{Foxp3-/-}$C57BL/6J) were purchased from Jackson Labs (Bar Harbor, Maine, USA). The mouse H22 hepatoma and S180 sarcoma cell lines were purchased from Guangdong Medical Experimental Animal Center (license no. scxk (Guangdong) 2013-0034). The experiment was divided into an H22 liver cancer group and an S180 sarcoma group. Each group was divided into $^{Foxp3-/-}$C57BL/6J and C57BL/6J subgroups, with ten 6–8 week old mice in each group (half males and half females). The mice were housed in a specific-pathogen-free (SPF) animal laboratory. Mice were housed in a controlled environment (22 °C, 50 ± 5% relative humidity, and 12-h light-dark cycle) and had free access to food and water. Laboratory animals were managed in accordance with the guidelines of the eighth edition of the Guidelines for the Care and Use of Laboratory Animals [23]. The aim of this study was to reduce the number and suffering of the experimental animals. The study was approved by the ethics committee of Guangdong Pharmaceutical University, China (approval no. GDPU-lal-2020,113).

For the H22 liver cancer group, *Foxp3* knockout and C57BL/6J mice were inoculated with H22 cells to grow the transplanted tumors. The numbers of splenic $CD4^+CD25^+Foxp3^+$T cells were determined by flow cytometry, and serum IL-10 and TGF-β1 levels were detected using a Luminex liquid suspension chip. Expression of *Foxp3* and lncRNA HULC in the microenvironment of the transplanted liver cancer was detected via FISH, and the relationship between *Foxp3* and HULC was analyzed [24].

For the S180 sarcoma group, *Foxp3* knockout and C57BL/6J mice were inoculated with S180 sarcoma cells to grow transplanted

tumors. The numbers of splenic $CD4^+CD25^+Fxop3^+$T cells were detected by flow cytometry, and serum IL-10 and TGF-β1 levels were assessed using a Luminex liquid suspension chip. Expression of *Foxp3* and HULC in the TME was detected via FISH to verify the relationship between *Foxp3* and HULC. This study conforms to the ARRIVE 2.0 guidelines [25].

2.3. Instruments and reagents

Bovine serum albumin (BSA), protease K, and 4′,6-diamidino-2-phenylindole (DAPI) were obtained from Wuhan Servicebio Company, China. Anti-DIG-HRP was provided by Jackson Corporation (PA, USA). CD4 (FITC), CD25 (PE-A), and Foxp3 (APC) were purchased from eBioscience (San Diego, CA, USA). PD-1, IL-10, TGF-β1, and Ki67 immunohistochemical kits were purchased from Fuzhou Maixin Biotechnology (Fujian, China).

A suspension bead chip platform (Luminex ® 200 ™) was used for performing. In situ fluorescence microscopy was performed using Nikon eclipse Ci (Nikon, Japan) and Nikon ds-u3 (Nikon, Japan). FACS Aria (BD company, USA) was used for flow cytometry. In situ hybridization slide (Servicebio Corporation, Wuhan, China), gene tech pen (Genentech, Inc., Southern California, USA), vortex mixing (Servicebio Corporation, Wuhan, China), and embedding machine (Wuhan Junjie Electronics Co., Ltd, China).

2.4. Model building

Establishment of the H22 hepatoma transplanted tumor model and S180 transplanted tumor model. After resuscitation, 0.1 ml H22 or S180 cells (1×10^7/ml) were subcutaneously injected into the left chest of mice. The transplanted tumor was formed after 3 days and detected after 14 days. On the 14^{th} day, mice were anesthetized with pentobarbital sodium 45 mg/kg via intraperitoneal injections and the mice were sacrificed for the experiment.

2.5. Flow cytometry

Flow cytometric detection of $CD4^+CD25^+Foxp3^+$T cells. The lymphocytes were separated via splenic shearing. Approximately 2 ml of the erythrocyte lysate was added for 2 min. Thereafter, the cell suspension was slowly added to the lymphocyte separation solution and centrifuged, and the lymphocytes in the middle layer were centrifuged for 15 min. The lymphocytes were adjusted to a concentration of 2×10^6/ml in 1640 culture medium and treated with PMA, iionomycin, or monensinibfa; 4 μl each. The mixture was then incubated at 37 °C for 6 h. Thereafter, 1.25 μl of CD25 FITC was added to each sample. The samples were then incubated with 1.25 μl anti-CD4 PE-A and 1.25 μl anti-FOXP3 PE-CY7-A antibodies for 30 min in the dark at 25 °C, and analyzed on Flow Analyzer. Another sample was obtained with CD90-FITC as a positive control.

2.6. FISH

Digoxin content in paraffin sections of FISH. Paraffin sections were dewaxed in water, digested, pre-hybridized, and the pre-hybridized solution was added dropwise, and incubated at 37 °C for 1 h. The probe containing the hybridizing solution was added dropwise at a concentration of 6 ng/μl and hybridization was performed at 37 °C in an incubator overnight. BSA was used as the blocking solution and added dropwise. Anti digoxin labeled peroxidase (anti dig HRP) was added dropwise. CY3-TSA reagent was added dropwise and reacted at 25 °C, in the dark, for 5 min. The nuclei were stained with DAPI and took photographs for microscopic examination. After taking pictures, the three fluorescence channels were superimposed using the image analysis software. Yellow fluorescence indicates that HULC gene and FOXP3 gene are co-localized. Results were analyzed using the following criteria: the presence of >15% positive cells among 200 tumor cells was recorded as low expression, whereas that of ≥30% qualified as high expression. The gene probes used are listed in Table 1.

2.7. IHC

IHC analysis was performed using a fully automatic immunostainer (DAKO Autostainer Link48). EnVision staining method. Ethylene diamine tetraacetic acid (EDTA) - high-temperature and high-pressure antigen retrieval method. Diaminobenzidine (DAB) color development method. Staining steps, EnVision two-step method, 4 μm thick serial sections, routine dewaxing, and hydration, EDTA (pH 9.0) pressure cooker water bath repair for 3 min, and natural cooling to 25 °C. The sections were incubated with hydrogen peroxide for 10 min at 25 °C to remove the endogenous peroxidase. The sections were treated with a primary antibody at a working concentration of 1:100, incubated at 25 °C for 60 min, rinsed with phosphate buffered saline (PBS) three times for 3 min each.

Table 1
Probe.

Foxp3 (red)	5′-DIG-GGGTG GTTTC TGAAG TAGGC GAACA TGCG-DIG-3′
Foxp3 (blue)	5′-DIG-GCAGACTCAGGTTGTGGCGGATGGCGTT-DIG-3′
IL-10 (red)	5′-DIG-TGGCC GACTG GGAAG TGGGT GCAGT TAT-DIG-3′
TGF-β1(red)	5′-DIG-CGGGC GTCAG CACTA GAAGC CACGG GAGT-DIG-3′
LncRNA HULC(red)	5′-DIG-TTCCTGCATGGTCTGGTTCTCGTGACGACTCTTCC T-DIG-3′

Thereafter, the sections were incubated in secondary antibodies (enzyme-labeled goat anti-mouse/rabbit IgG polymer) at 25 °C for 30 min, washed with PBS three times for 3 min each. DAB was used for color development and hematoxylin for contrast staining. Neutral gum was used for sealing the piece. PBS was used as a negative control.

Determining PD-1 positivity. PD-1 is localized on the cell membrane and partly in the cytoplasm. A brown-yellow staining signal under the low magnification microscope >1% was classified as positive (the number of cytoplasmic positive cells of any intensity/the number of cells in the whole film) and <1% as negative. A value ≥ 50% was considered strongly positive. PD-1 expressing lymphocytes were differentiated from tumor cells using the following criteria: Lymphocytes were identified as diffusely distributed small cells with only nuclei and no cytoplasm. Tumor cells were defined as nested aggregates with large nuclei, three times greater than that of lymphocytes.

Positive scoring for IL-10 and TGF-β1 levels. IL-10 positive expression is located in the nucleus. TGF-β1 was localized on the cell membrane and in the cell cytoplasm. IL-10 and TGF-β1 expression was determined by multiplying the intensity of cell staining with the percentage of positive cells. The average optical density values were analyzed using an image analysis software. Staining intensity was scored as per the following criteria, 0 for no staining, 1 for light yellow, 2 for tan, and 3 for brown tan. The percentage of the visual field occupied by stained cells was scored by taking five consecutive high-power visual fields under a 400-fold optical microscope for each section and taking the mean value. Positive cell rate: 0 points for <5%, 1 point for 5–25%, 2 points for 25–50%, 3 points for 50–75%, and 4 points for >75%. The two values were multiplied to obtain the final score: 0–2, negative (−), 3–4 is weakly positive (+), 5–8 is moderately positive (++), 9–12 is strong positive (++ +).

2.8. Enzyme-linked immunosorbent assay

Enzyme-linked immunosorbent assay (ELISA) was used to detect the concentrations of IL-10 and TGF-β1 in the serum samples of the patients. The standards and 40 μl of diluted samples were added to the 96-well plates. Subsequently, 25 samples were tested. The mixture was then incubated at 37 °C for 30 min. After washing, 50 μl of the enzyme-labeling reagent was added to the wells. The plates were incubated at 25 °C for 30 min. Following color development, the reaction was terminated using a stop solution. The plates were incubated for 50 min and the absorbance was measured at 450 nm.

Cytokine concentrations in animal sera were detected using a Luminex liquid suspension chip. The samples were incubated at room temperature in the dark for 120 min. Following incubation, 50 μl of diluted detection antibody was added to each well and the samples incubated at 25 °C, in the dark, for 60 min. The detection antibody was discarded after color development and the samples were washed three times with PBS. Thereafter, 50 μl of diluted streptavidin-PE was added to each hole before incubation at 25 °C, in the dark, for 30 min. Next, 100 μl of was added to each hole to suspend the wash buffer. After applying the sealing film and oscillate at 25 °C in the dark, for 2 min, the results were collected using a corrected Luminex 200 machine.

2.9. Statistical methods

The experimental results were analyzed using the statistical software SAS8.2 (SAS Software Corporation, USA), and the data are expressed as the mean ± standard deviation (x ± s). If the measured data conformed to a normal distribution and exhibited homogeneity in variance, an independent sample *t*-test or one-way analysis of variance was performed. Morphological data are expressed as median ± interquartile range. If the normal distribution and unequal variance were not satisfied simultaneously, the Wilcoxon rank sum test was used for analysis. The chi-square test was used for nonparametric multiple group comparisons. Flow cytometry data were analyzed using FlowJo software V10.0 (BD Biosciences, USA) Statistical analysis of cytokines was performed with GraphPad Prism 8.2.1 (GraphPad Software, USA). Statistical significance was set at $p < 0.05$.

Table 2
Clinical data.

	HCC	Colon cancer liver metastasis	sarcoma
old (mean ± SD)	47.7 ± 12.2	52.6 ± 10.5	55.5 ± 11.2
sex			
man	21(70%)	19(63.3%)	18(56.2%)
woman	9 (30%)	11(36.7%)	14(43.8%)
Tumor size			
T1	4(13.3%)	5(16.7%)	1(3.1%)
T2	6(20%)	7(23.3%)	3(9.4%)
T3	9(30%)	8(26.7%)	13(40.7%)
T4	11(36.7%)	10(33.3%)	15(46.8%)
Lymph node			
N0	6(20%)	5(16.7)	3(9.4%)
N1	15(50%)	16(53.3%)	0(0%)
N2	5(16.7%)	4(13.3%)	0(0%)
N3	4(13.3)	5(16.7)	0(0%)
Distant metastasis	13(43.3%)	30(100%)	14(43.8)

Note: T is the degree of tumor invasion, and the stages are from T1 to T4. N is a lymphoid metastatic condition, at stages N0 to N3.

3. Results

3.1. LncRNA HULC promotes treg cell differentiation and immune escape

Table 2 represents the clinical data for the 30 HCC, 30 colon cancer liver metastases, and 32 sarcoma cases that were included in this study. The pathological diagnosis of malignant tumors was clear.

Both *FOXP3* gene and *HULC* gene were highly expressed in sarcoma specimens (Fig. 1A), and *FOXP3* gene and *HULC* gene were also highly expressed in liver metastases from colon cancer patients (Fig. 1B). Expression of the *FOXP3* gene and the *HULC* gene appeared in the HCC specimens (Fig. 1C). The results of the statistical analysis of each group have been presented in Fig. 1D. Fluorescent staining, DAPI nuclei (blue), *FOXP3* (green), LncRNA *HULC* (red). *FOXP3* and LncRNA *HULC* were clearly visible in the cytoplasm after Merge. Local magnification of each group showed that the *FOXP3* and *HULC* genes coincided completely (Fig. 1E). The results showed that within the TME, the cancer cell lncRNA HULC promoted gene expression in Treg cells.

3.2. LncRNA HULC promote the increase of cytokines IL-10 and TGF-β1 in the TME

The expression of FOXP3 over 50% resulted in an increased expression of IL-10 and TGF-β1 for the HCC specimens (Fig. 2A and B).

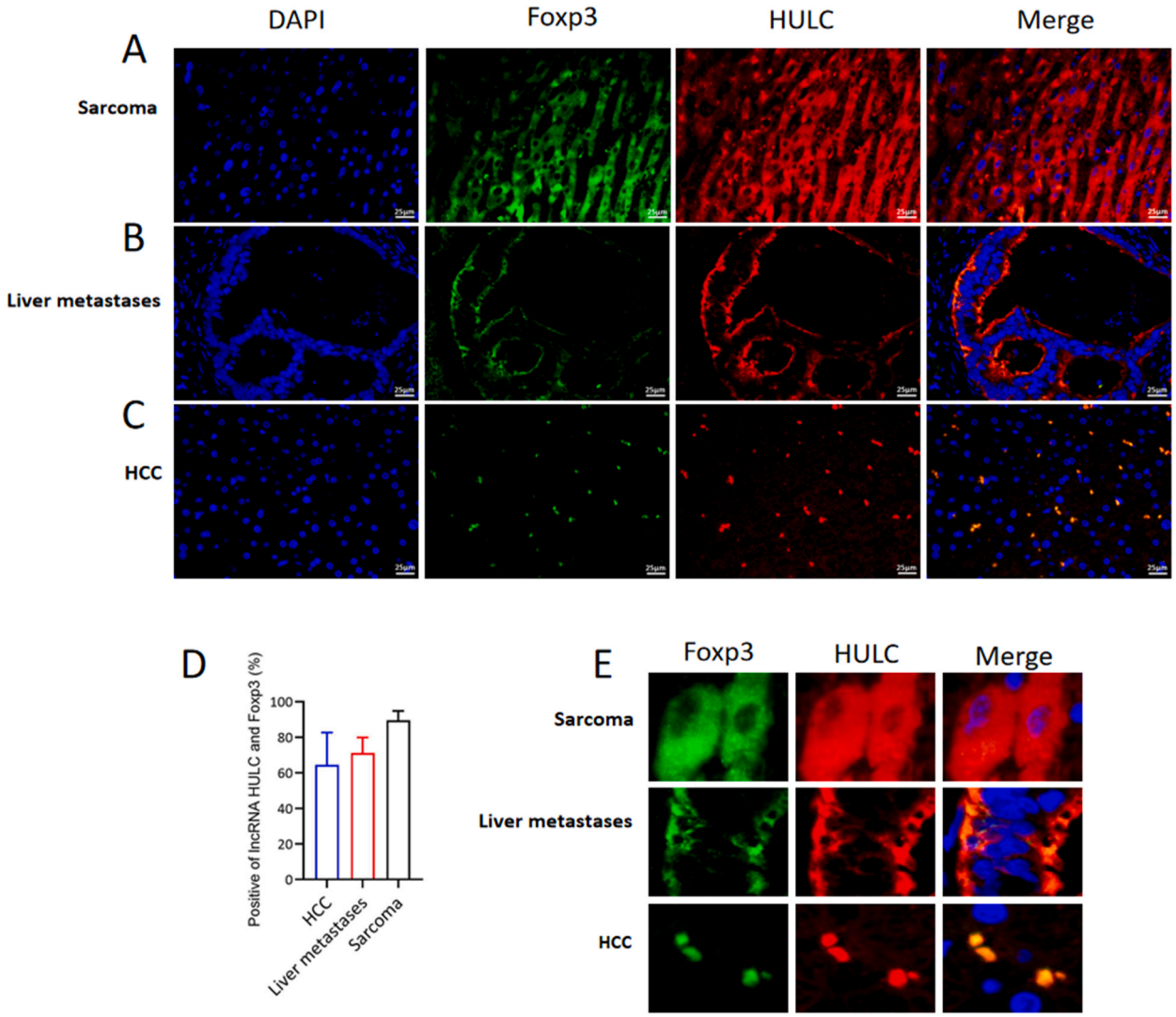

Fig. 1. The *HULC* gene in cancer cells promotes Tregs expression in the TME. A In the sarcoma microenvironment, the pression of *FOXP3* (green) gene is 89.6 ± 5.12%, and lncRNA *HULC* (red) genes is 86.2 ± 8.67%. B In colon cancer liver metastases, the pression of *FOXP3* (green) gene was 73.07 ± 8.69%, and lncRNA *HULC* genes is 71.2 ± 7.02%. C For HCC specimens, the gene expression rate of FOXP 3 was 35.24 ± 7.23%, and the HULC gene was 31.04 ± 5.23%. D Statistical analysis for each group. E High expression of the *FOXP3* and lncRNA *HULC* genes (Bright yellow).

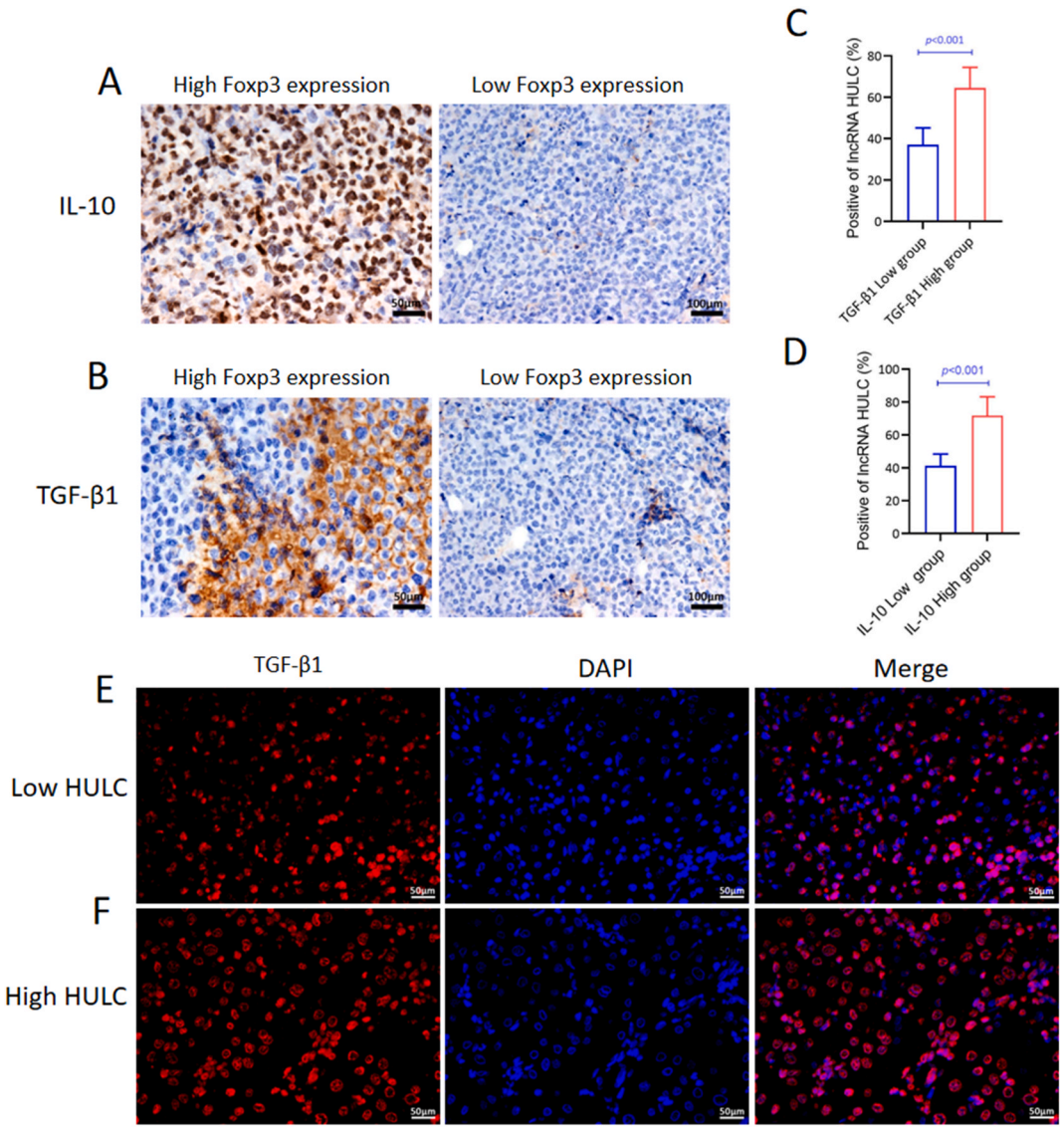

Fig. 2. lncRNA HULC promotes IL-10 and TGF-β1 expression within the TME of poorly differentiated HCC. A IL-10 positive was located in the nucleus of HCC specimens. Increased expression of Foxp3 results in IL-10 upregulation. IL-10 in 30 HCC specimens, 2+ positive was 12 and 13+ positive 11. B IL-10 expression in the HCC specimens is reduced when Foxp3 levels decrease. C When Foxp3 is upregulated, the expression of TGF-β1 increases, and indicated by the presence brownish yellow fluorescence, which is located on the plasma membrane and partly in the cell cytoplasm. TGF-β1 in 30 HCC specimens, 2+ positive was 14 and 3+ positive was 10. D TGF-β1 expression is reduced with a decrease in Foxp3 expression in the HCC specimens. E An increase in TGF-β1 expression corresponded with a subsequent increase in lncRNA HULC expression ($p < 0.001$). F High IL-10 expression was associated with increased expression of lncRNA HULC ($p < 0.001$). G In the TME, the expression of IL-10, TGF-β1, and lncRNA HULC was decreased. H lncRNA HULC levels increased when the HCC specimens were TGF-β1 positive.

High expression of lncRNA HULC (≥50%) was associated with an increase in TGF-β1 levels. Conversely, low lncRNA HULC expression (<50%) was associated with a decrease in TGF-β1 levels, $p < 0.001$ (Fig. 2C–E, and F). Next, high expression of the lncRNA HULC (≥50%) was also associated with an increase in IL-10 levels. In contrast, low lncRNA HULC expression was associated with a decrease in IL-10 levels (<50%), $p < 0.001$, (Fig. 2D). These results suggest that lncRNA HULC expression within the liver cancer tissue mediated an increase in IL-10 and TGF-β1 levels.

3.3. Treg cells promote PD-1 expression within the TME

We analyzed the relationship between PD-1 and the Treg cells within the TME of poorly differentiated HCC. Our results showed that the number of $CD4^{+}CD25^{+}Foxp3^{+}$T cells in the serum of HCC patients was higher than that in the serum of the control group ($p < 0.01$) (Fig. 3A and B). The serum concentrations of TGF-β1 and IL-10 were higher ($p < 0.001$) in the liver cancer group than in the

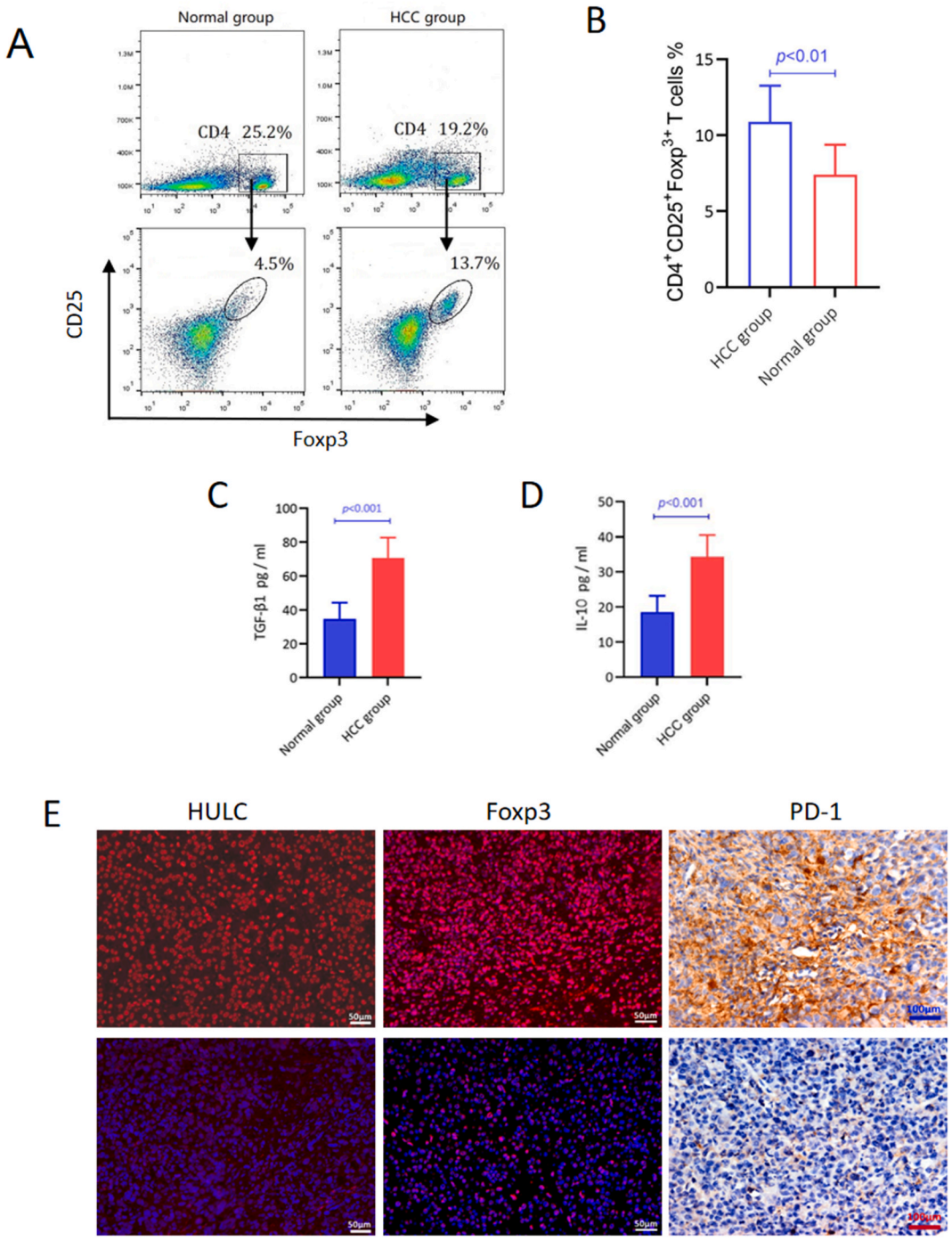

Fig. 3. Treg cells promote the increase in PD-1 expression in TME of HCC. A There was an increase in the number of $CD4^{+}CD25^{+}Foxp3^{+}$ T cells in the serum of patients from the HCC group. B The liver cancer group had 10.82 ± 2.17% ($p < 0.01$) Treg cells, whereas the number of Treg cells in the normal group was 7.38 ± 1.84% ($p < 0.01$). C The concentration of TGF-β1 in the serum of patients with liver cancer increased ($p < 0.001$). D The concentration of serum IL-10, was higher in the liver cancer group than in the normal group ($p < 0.001$). E lncRNA HULC (red), Foxp3 (red) and PD-1 expression increased; when lncRNA HULC decreased, Foxp3 and PD-1 expression also decreased in the tumor microenvironment of HCC. PD-1 positivity (brownish yellow) in HCC specimens was determined, × 40. PD-1 is expressed in the cell membrane of malignant cells. Of the 30 HCC specimens, nine were 2+ positive and eight were 3+ positive.

control group (Fig. 3C and D). lncRNA HULC, Foxp 3 and PD-1 expression increased; when lncRNA HULC decreased, Foxp3 and PD-1 expression also decreased in the tumor microenvironment of HCC (Fig. 3E). This indicated that cancer cells promoted the secretion of TGF-β1 and IL -10 by Treg cells. The results of this study showed that *FOXP3* promoted the increase in PD-1 expression in the TME.

3.4. Treg cells promote PD-1 expression in the TME of transplanted H22 liver cancer

Tregs promote the expression of PD-1 in the TME of H22 liver cancer. We analyzed the lymphocyte numbers in the spleens of Foxp3

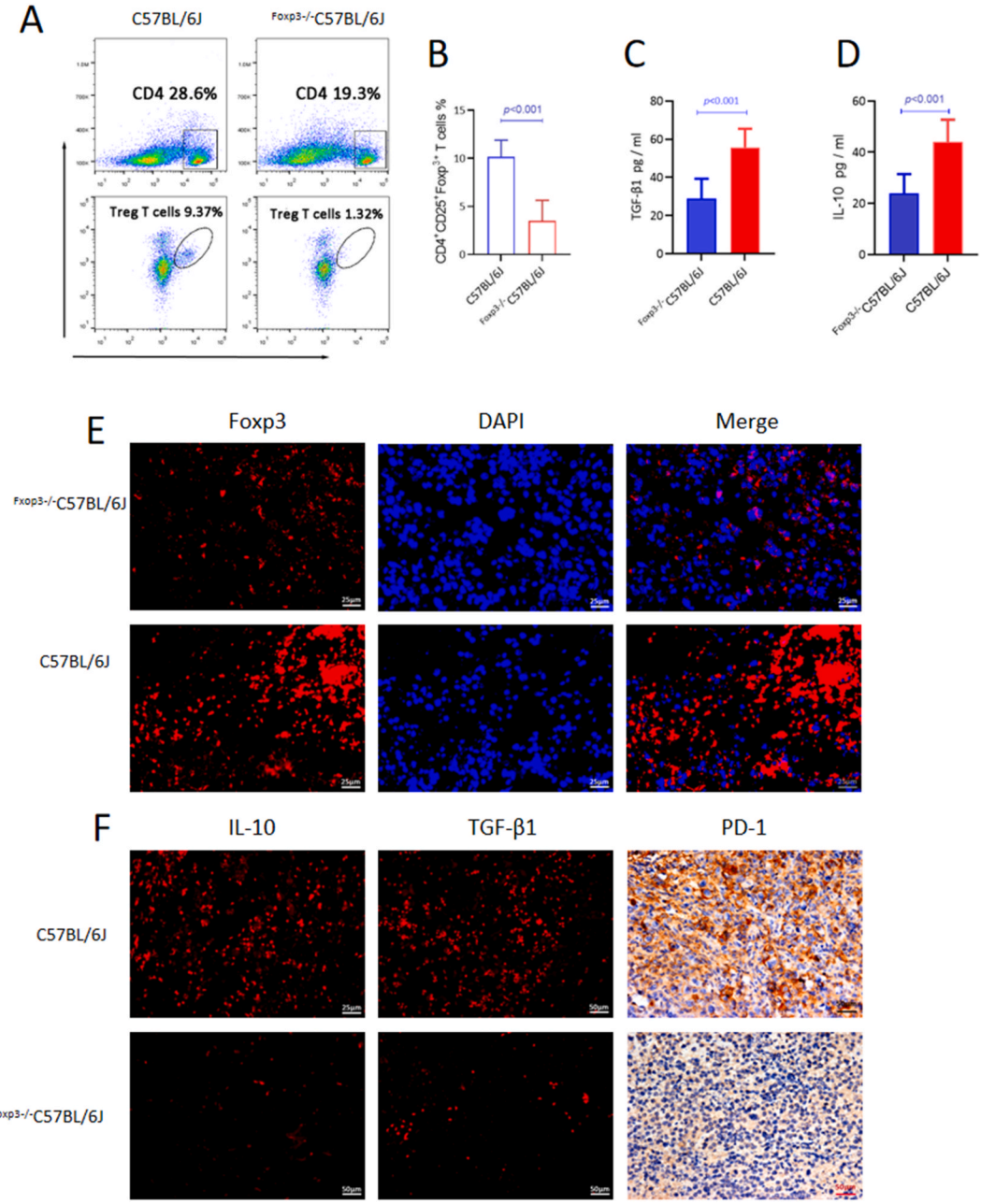

Fig. 4. Treg cells promote PD-1 expression in the H22 transplanted TME. A The number of splenic $CD4^+CD25^+Foxp3^+$T cells in the C57BL/6J group was 9.82 ± 3.2% and that in the *Foxp3* gene knockout group was 1.35 ± 0.8%. B Comparison of the two groups, $p < 0.001$. C Serum concentration of TGF-β1 was 55.65 ± 9.79% for the C57BL/6J group and 28.1 ± 10.48% for the *Foxp3* gene knockout group ($p < 0.001$). D Serum concentration of IL-10 was 44.2 ± 8.79% for the C57BL/6J group and 23.99 ± 7.46% for the *Foxp3* gene knockout group ($p < 0.001$). Foxp3 gene knockout group H22 TME and decreased Foxp3 gene expression. In the Foxp3 knockout group, the expression of the *Il10, Tgfb1*, and PD-1 decreased in H22 liver cancer. PD-1 is expressed on the membranes of tumor cells. Among the 10H22 liver cancers, three were 2+ positive and four were 3+ positive.

knockout and C57BL/6J mice, and detected 1.35 ± 0.8% and 9.25 ± 2.1% $CD4^{+}CD25^{+}Foxp3^{+}$T cells, respectively ($p < 0.001$; Fig. 4A and B). In the $^{Foxp3-/-}$C57BL/6J group, serum IL-10 and TGF-β1 concentrations decreased, indicating that Treg cells were secreting IL-10 and TGF-β1 (Fig. 4C and D). In the TME of the transplanted tumor, expression of the *FOXP3* gene was significantly reduced in the $^{Foxp3-/-}$C57BL/6J group compared to that in the C57BL/6J group (Fig. 4E). The expression of *Il10, Tgfb1* and PD-1 was lower in the $^{Foxp3-/-}$C57BL/6J group than in the C57BL/6J group (Fig. 4G and F).

3.5. Inhibiting the lncRNA HULC-Treg-PD-1 axis limits immune escape

Knocking out the *Foxp3* gene can inhibit the lncRNA HULC-Treg-PD-1 pathway. We recorded significant reduction in the size and growth of the H22 transplanted tumors. Specifically, the size of the H22 transplanted tumors in mice from the $^{Foxp3-/-}$C57BL/6J group was significantly smaller compared to those in mice from the C57BL/6 group ($p = 0.002$) (Fig. 5A and B). Compared to the C57BL/6J

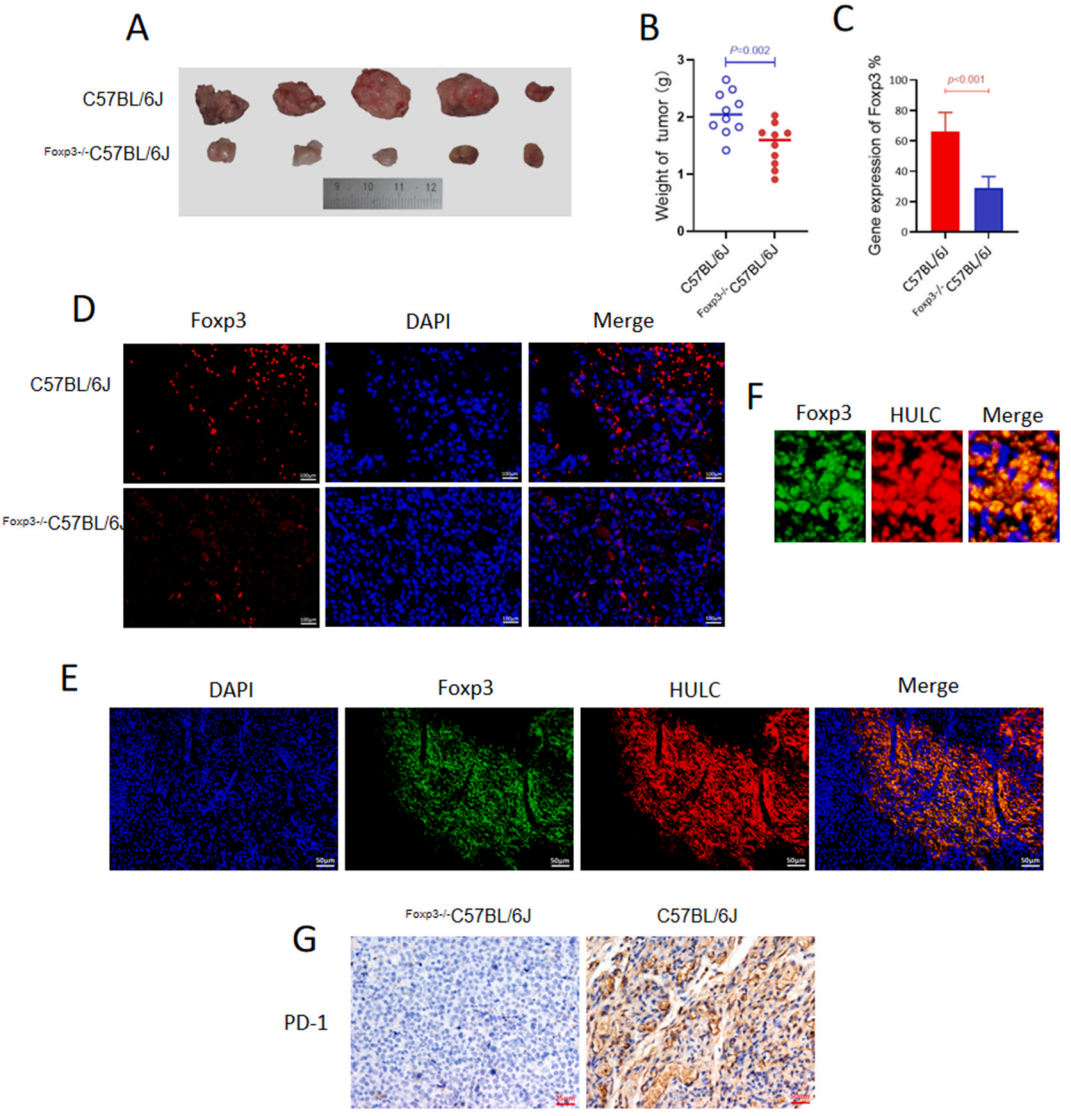

Fig. 5. Knocking out the *Foxp3* gene can reduce the expression of lncRNA HULC and inhibit the growth of the transplanted H22 tumors. A H22 cells were inoculated into C57BL/6J and $^{Foxp3-/-}$C57BL/6J mice, and the transplanted tumors were formed in 14 days. The transplanted tumors were significantly smaller in mice from the $^{Foxp3-/-}$C57BL/6J group than in mice from the C57BL/6J group. B The weight of the transplanted tumor in the C57BL/6J group was 2.07 ± 0.56 g, whereas that in the $^{Foxp3-/-}$C57BL/6J group was 1.51 ± 0.48 g ($p = 0.002$). C In the C57BL/6J group, the positive expression of lncRNA HULC was 66.28 ± 12.44%, whereas that in the $^{Foxp3-/-}$C57BL/6J group was 28.91 ± 7.57% ($p < 0.001$). D *Foxp3* expression in the H22 transplanted tumor. E *Foxp3* and *HULC* genes are overlap completely in the transplanted tumors. F Strong overlap between the *Foxp3* and *HULC* genes. G PD-1 is expressed on the cell membrane of H22 cells. Among the 10H22 liver cancer samples, four were 2+ positive and three were 3+ positive.

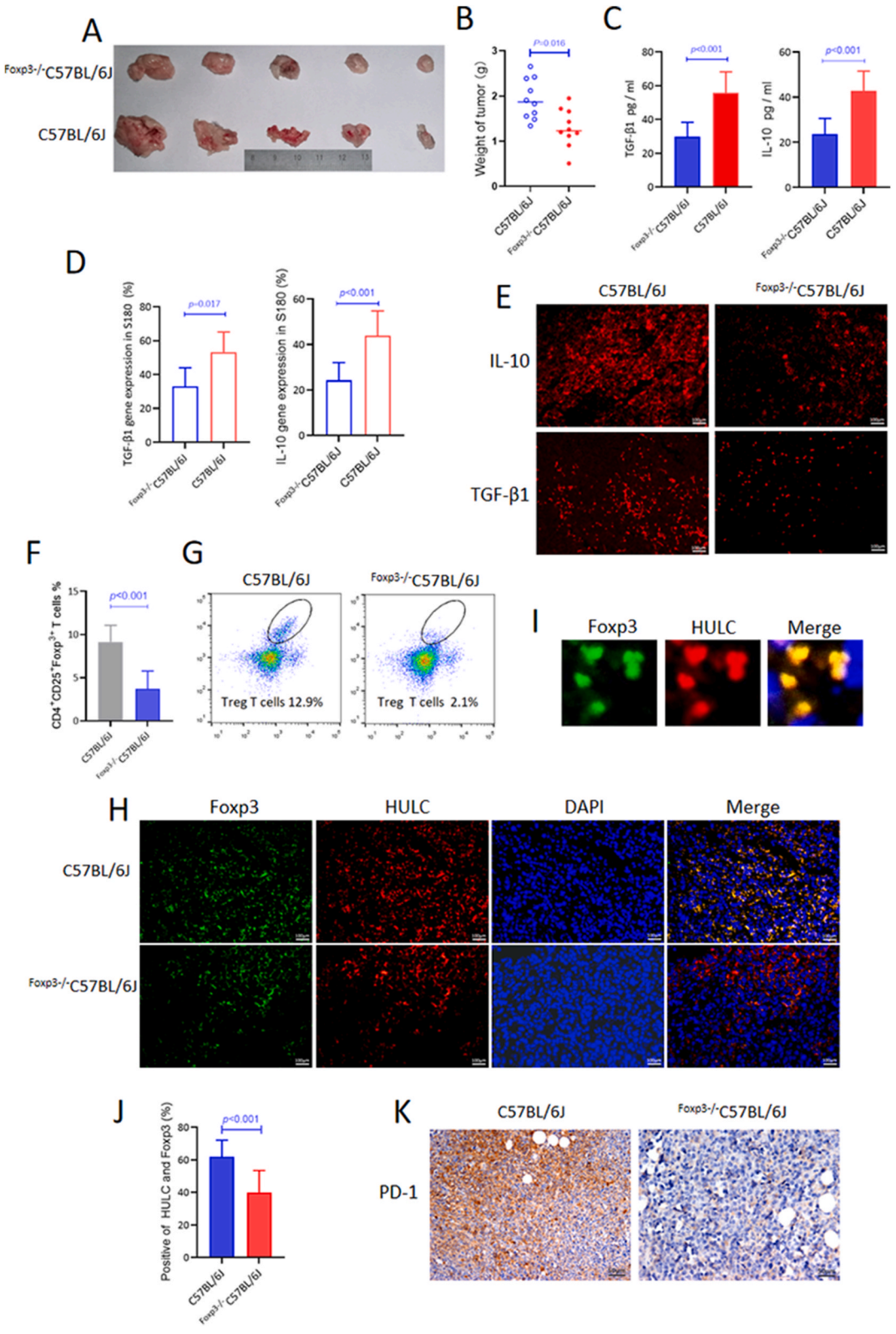

(caption on next page)

Fig. 6. Knocking out *Foxp3* can reduce the expression of lncRNA HULC and control the sarcoma growth. A S180 sarcoma cells were inoculated into C57BL/6J and $^{Foxp3-/-}$C57BL/6J mice. After 14 days, transplanted tumors were formed. There was a significant reduction in the size of transplanted tumors in mice from the $^{Foxp3-/-}$C57BL/6J group. B The weight of the transplanted tumor in the C57BL/6J group was 1.933 ± 0.63 g, and whereas that for tumors from the $^{Foxp3-/-}$C57BL/6J group was 1.29 ± 0.62 g ($p = 0.016$). C Serum concentration of TGF-β1 in the C57BL/6J and $^{Foxp3-/-}$C57BL/6J groups was 55.75 ± 12.47 pg/ml and 29.88 ± 8.39 pg/ml, respectively ($p < 0.001$). Serum concentration of IL-10 was 42.83 ± 8.69 pg/ml and 23.61 ± 6.91 pg/ml for the C57BL/6J and $^{Foxp3-/-}$C57BL/6J groups, respectively ($p < 0.001$). D In the sarcoma TME, *Tgfb1* expression in the C57BL/6J group was 53.21 ± 11.91%, whereas that in the $^{Foxp3-/-}$C57BL/6J group was 33.03 ± 10.91% ($p < 0.001$). The expression of *Il10* in C57BL/6J group was 43.86 ± 10.93%, whereas that in $^{Foxp3-/-}$C57BL/6J group was 24.27 ± 7.76% ($p < 0.001$). E In S180 sarcoma transplanted tumors, the incidence of *Foxp3* and *HULC* genes in mice from the C57BL/6J and $^{Foxp3-/-}$C57BL/6J groups was 61.97 ± 10.2% and 40.07 ± 13.35%, respectively ($p < 0.001$). F Concentration of Treg cells was 9.15 ± 5.43% in the C57BL/6J group and 3.71 ± 1.02% in the $^{Foxp3-/-}$C57BL/6J group ($p < 0.001$). G There was a significant reduction in the number of $CD4^+CD25^+Foxp3^+$T cells in the spleens of *Foxp3* knockout mice. H In S180 sarcoma, *Foxp3* and *HULC* genes are expressed consistently. (× 40). I The *Foxp3* and *HULC* genes overlap highly. J Statistical analysis for the two groups. K PD-1 is expressed on the cell membrane of S180 transplanted tumors. Among the ten S180 sarcomas, four were 2+ positive and three were 3+ positive.

group, *HULC* gene expression in the $^{Foxp3-/-}$C57BL/6J group was significantly reduced ($p < 0.001$; Fig. 5C), indicating that Treg cells promoted the expression of lncRNA HULC (Fig. 5D). The *FOXP3* gene overlapped and co-localized with the *HULC* gene in the TME (Fig. 5E). There was a strong overlap between the *FOXP3* and *HULC* genes when the local area was enlarged (Fig. 5F). Compared to the C57BL/6J group, PD-1 expression in the transplanted tumors in the $^{Foxp3-/-}$C57BL/6J group was significantly reduced ($p < 0.001$; Fig. 5G). Together, the results for these experiments show that controlling the lncRNA HULC-Treg-PD-1 pathway can inhibit the growth of transplanted H22 tumors.

3.6. Regulating the lncRNA HULC-Treg-PD-1 axis to inhibit the growth of the sarcoma

Knocking out the *Foxp3* gene can inhibit the effects of the lncRNA HULC-Treg-PD-1 pathway in the TME of S180 transplanted tumors and control sarcoma growth. The weight of transplanted S180 sarcoma tumors significantly decreased in the $^{Foxp3-/-}$C57BL/6J group (Fig. 6A) compared to that in the C57BL/6 group ($p = 0.016$; Fig. 6B). Additionally, serum concentrations of IL-10 and TGF-β1 were significantly lower in mice from the $^{Foxp3-/-}$C57BL/6J group than in mice from the C57BL/6J group ($p < 0.001$; Fig. 6C). In the TME of the S180 transplanted tumor, the expression of *Il10* ($p < 0.001$) and *Tgfb1* ($p = 0.017$) was lower in the $^{Foxp3-/-}$C57BL/6J group than in the C57BL/6J group (Fig. 6D). Knocking out *Foxp3* caused a significant reduction in the expression of *Il10* and *Tgfb1* in the transplanted tumors (Fig. 6E). In *Foxp3* knockout mice, the detection rate of $CD4^+CD25^+Foxp3^+$T cells was significantly lower than that in the C57BL/6J group, ($p < 0.001$; Fig. 6F and G). Foxp3 expression was significantly lower in the $^{Foxp3-/-}$C57BL/6J group than that in the C57BL/6J group. We observed an overlap between the *Foxp3* and *HULC* genes (Fig. 6H), and the local enlargement showed that the *Foxp3* gene and the lncRNA *HULC* gene overlapped completely(Fig. 6I). Compared to the C57BL/6J group, PD-1 protein expression in the H22 liver cancer was significantly reduced in the $^{Foxp3-/-}$C57BL/6J group ($p < 0.001$). The co-expression rate of the Foxp3 gene and the lncRNA HULC gene was lower in the $^{Foxp3-/-}$C57BL/6J group than in the C57BL/6J group ($p < 0.001$; Fig. 6J). PD-1 protein expression was significantly lower in the sarcoma of the $^{Foxp3-/-}$C57BL/6J group ($p < 0.001$; Fig. 6K) than in that of the C57BL/6J group. Collectively, our results showed that modulating the lncRNA HULC-Treg-PD-1 pathway could affect the growth of S180 sarcoma.

4. Discussion

The lncRNA promotes an increase in the number of Tregs and facilitates immune escape in the TME [26,27]. LncRNAs plays an important role in cancer development. They participate in epigenetic, transcriptional, and post-transcriptional regulation through various chromatin-based mechanisms and interactions with different types of RNA [28]. As a downstream effector of the TGF-β signaling pathway, the lncRNA-p21 interacts with miR-30 in liver cells to enhance the TGF-β signaling pathway and promote liver fibrosis [29]. Compared to healthy controls, there was a significant increase in the serum levels of IL-10, IL-17, and lncRNA-AF085935 in patients with HCV-associated rheumatoid arthritis [30]. Reducing IL-10 and vascular endothelial growth factor-A (VEGF-A) levels can inhibit tumors caused by lncRNA GAS5 proliferation [31]. In HCC, the proliferation, differentiation, migration, and effector functions of Treg cells have been associated with a poor prognosis [32]. However, Treg cells cannot be treated with targeted or immune drugs [33]. These results indicated that the role of Treg cells in the TME requires further research.

The interaction between lncRNA HULC, rs1041279 SNP, and rs2038540 SNP and the environmental factors can increase the risk of HCC [34] and promote the development of liver cancer. It is believed that the prognosis is poor [35] and lncRNA HULC can be used as a new marker for liver cancer [36]. The present data shows that the *Foxp3* and *HULC* genes overlap highly in soft tissue sarcoma, colon cancer, liver metastasis, and HCC. Expression of the *Foxp3* and HULC genes also highly overlaps in the TME of mice with H22 liver cancer and S180 sarcoma, indicative of an important interaction between the two genes. In the transplanted tumor microenvironment of *Foxp3* knockout mice, it is important to directly discuss the effect and mention the measured quantity that reflected the weakening, indicating that the lncRNA HULC regulates Treg cells.

An increase in Treg cells leads to an increase in PD-1 levels in the TME. In HCC with HBsAg positivity and *Foxp3* gene expression, the degree of malignancy was higher. Compared to healthy individuals, there was an increase in the numbers of Treg cells, myeloid-derived suppressor cells (MDSC), and PD-1(+) exhausted T cells and the levels of immunosuppressive cytokines in patients with HCC

[37]. Our data shows that in the liver cancer microenvironment, where the *Foxp3* gene is highly expressed, the expression of IL-10 and TGF-β1 increases significantly, indicating that Treg cells mainly act through IL-10 and TGF-β1.

PD-1 plays an important role in suppressing immune responses and promoting self-tolerance by regulating the activity of T cells, for example, by activating apoptosis of antigen-specific T cells and inhibiting apoptosis of Treg cells [38]. In highly advanced gastric cancer, PD-1 may promote the proliferation of highly suppressed PD-1^{+} effector regulatory T cells (eTreg cells), thereby inhibiting antitumor immunity [39]. The PD-1/PD-L1 axis-blockade therapy is a promising treatment alternative, which has significant clinical benefits for several types of tumors [40]. Our study shows that an increase in Treg cells can lead to an increase in the levels of PD-1 in the TME, a receptor that exerts immunosuppressive effects. The expression of PD-1 can be reduced by knocking out the *Foxp3* gene.

In liver cancer specimens, lncRNA HULC increased the levels of IL-10 and TGF-β1 in Treg cells. Treg cells mainly secrete IL-10 and TGF-β1, which plays important roles in HCC [41]. The combined use of IL-10 and TGF-β1 can limit T cell responses to heterologous antigens, inhibit the antigen-specific immune response to allogeneic liver antigens, prolong the survival of allogeneic liver, and enhance immune tolerance; but has an unfavorable effect on HCC treatment [42]. Our results show that the lncRNA HULC increases the levels of IL-10 and TGF-β1 in Treg cells and has an immunosuppressive effect in the TME.

Knocking out *FOXP3* inhibits the lncRNA HULC-Treg-PD-1 axis and controls immune escape. Tregs lead to an immunosuppressive state in the TME. When considering cancer immunotherapy, it is important to overcome the Treg-mediated immune tolerance [43]. Clinical studies on therapeutics mediating Treg cell depletion and targeting the anti-tumor functions Treg cells have been performed in the past; however, these treatments cannot selectively deplete or inhibit Treg cells, especially tumor-infiltrating Treg cells [44,45]. After the rat Carma-bcl10-malt1 (CBM) signal body complex is destroyed, most tumor-infiltrating Treg cells produce interferon-γ, leading to tumor growth inhibition. Therefore, single-agent anti-PD-1 therapy is ineffective, CBM complexes can become therapeutic targets for immune checkpoints [46], and PD-1 inhibitors alone have poor therapeutic effects.

Treg cells infiltration may be a physiological response to limit inflammation in the TME. Blocking the pathways that stabilize Treg cells can increase the sensitivity of tumors to radiotherapy and chemotherapy, and enhance the antitumor immune response [47]. However, the present methods that target Treg cells still have serious side effects [48], and further research on Treg cell functions and treatment alternatives for targeting Treg cells is needed. Our study showed that controlling the levels of Treg cells could restrict the lncRNA HULC-Treg-PD-1 pathway and inhibit the growth of malignant tumors.

Interfering with the lncRNA SNHG1 can inhibit the differentiation of Treg cells by promoting miR-448 expression and reducing indoleamine 2,3-dioxygenase (IDO) levels, thereby hindering immune escape during breast cancer [49]. miR-423-5p is highly expressed in HCC cells. Overexpression of lncRNA FENDRR and downregulation of miR-423-5p reduce HCC cells proliferation and tumorigenicity, promotes HCC cell apoptosis, and thereby miR-423-5p regulates Treg-mediated immune escape in liver cancer [50]. Circulating Treg cells and HULC are significantly upregulated in the plasma samples of patients with HBV-associated cirrhosis. Moreover, HULC can regulate the function of Treg cells by directly downregulating p18 levels [51]. LncRNA-POU3F3 can promote the distribution of Treg cells in peripheral blood T cells and enhance the proliferation of gastric cancer cells by recruiting TGF-β and activating the TGF-β signaling pathway [52]. Our study shows that collectively inhibiting the expression of lncRNA HULC, blocking the infiltration of Tregs in the TME, and controlling PD-1 protein may be a more effective treatment alternative.

5. Conclusion

In conclusion, high expression of *HULC* promotes the increased number of Treg cells and increases the expression of PD-1 in the TME. The lncRNA HULC-Treg-PD-1 axis has an immunosuppressive effect, and facilitates immune escape and tumor cell proliferation. Modulating the lncRNA HULC-Treg-PD-1 axis can reduce the expression of PD-1, decrease secretion of IL-10 and TGF-β1, and thereby limit the growth of malignant tumors. This study lacks the confirmation of lncRNA HULC gene knockout studies. The drug development of lncRNA HULC-Treg-PD-1 is the direction for future development.

Ethics approval and consent to participate

The study was approved by the ethics committee of Guangdong Pharmaceutical University, China (approval no. GDPULAL202020113).

Consent for publication

All researchers in this paper agree to publish this article.

Data availability statement

The authors will supply the relevant data in response to reasonable requests.

Funding

This work was supported by the Major Science and Technology Project of Guangzhou Panyu District (2017-z04-01,2018-z04-01).

CRediT authorship contribution statement

XiaoYu Wang: Writing – review & editing, Project administration. **Xiaoyan Mo:** Writing – original draft, Methodology, Investigation. **Zhuolin Yang:** Resources, Methodology, Investigation, Formal analysis, Data curation. **Changlin Zhao:** Writing – review & editing, Writing – original draft, Methodology, Funding acquisition, Formal analysis, Data curation.

Declaration of competing interest

The authors declare that they have no known competing financial interests or personal relationships that could have appeared to influence the work reported in this paper.

Acknowledgements

Not applicable.

Abbreviations

CBM	carma-bcl10-malt1
CREB	cyclic adenosine monophosphate response element binding protein
EDTA	ethylene diamine tetraacetic acid
ELISA	enzyme-linked immunosorbent assay
eTreg cells	effector regulatory T cells
Fish	fluorescence in situ hybridization
Foxp3	forkhead box P3
GCP	good clinical practice
HBx	hepatitis B virus X protein
HCC	hepatic carcinoma
HCV	hepatitis C virus
HULC	highly upregulated in liver cancer
IDO	indoleamine 2,3-dioxygenase
IHC	immunohistochemistry
IL-10	interleukin-10
lncRNAs	long non-coding RNAs
MSDC	myeloid-derived suppressor cells
PBS	phosphate buffered saline
PD-1	programmed death-1
PD-L1	programmed cell death ligand 1
TGF-β1	transforming growth factor β1
TLR8	toll-like receptors 8
TME	tumor microenvironment
Treg	regulatory T cell

References

[1] F. Lu, L. Hou, S. Wang, Y. Yu, Y. Zhang, L. Sun, et al., Lysosome activable polymeric vorinostat encapsulating PD-L1KD for a combination of HDACi and immunotherapy, Drug Deliv. 28 (1) (2021) 963–972.
[2] L. Göschl, C. Scheinecker, M. Bonelli, Treg cells in autoimmunity: from identification to Treg-based therapies, Semin. Immunopathol. 41 (3) (2019) 301–314.
[3] M. Nikolova, A. Wiedemann, M. Muhtarova, D. Achkova, C. Lacabaratz, Y. Lévy, Subset- and antigen-specific effects of Treg on CD8+ T cell responses in chronic HIV infection, PLoS Pathog. 12 (11) (2016) e1005995.
[4] Y. Furusawa, Y. Obata, S. Fukuda, T.A. Endo, G. Nakato, D. Takahashi, et al., Commensal microbe-derived butyrate induces the differentiation of colonic regulatory T cells, Nature 504 (7480) (2013) 446–450.
[5] N. Sepúlveda, J. Carneiro, E. Lacerda, L. Nacul, Myalgic encephalomyelitis/chronic fatigue syndrome as a hyper-regulated immune system driven by an interplay between regulatory T cells and chronic human herpesvirus infections, Front. Immunol. 10 (11) (2019) 2684.
[6] A. Carambia, B. Freund, D. Schwinge, O.T. Bruns, S.C. Salmen, H. Ittrich, et al., Nanoparticle-based autoantigen delivery to Treg-inducing liver sinusoidal endothelial cells enables control of autoimmunity in mice, J. Hepatol. 62 (6) (2015) 1349–1356.
[7] S.H. Park, N.S. Veerapu, E.C. Shin, A. Biancotto, J.P. McCoy, S. Capone, et al., Subinfectious hepatitis C virus exposures suppress T cell responses against subsequent acute infection, Nat. Med. 19 (12) (2013) 1638–1642.
[8] P. Lapierre, A. Lamarre, Regulatory T cells in autoimmune and viral chronic hepatitis, J Immunol Res 2015 (2015) 479703.
[9] S. Najafi, A. Mirshafiey, The role of T helper 17 and regulatory T cells in tumor microenvironment, Immunopharmacol. Immunotoxicol. 41 (1) (2019) 16–24.
[10] A.E. Overacre-Delgoffe, D.A.A. Vignali, Treg fragility: a prerequisite for effective antitumor immunity? Cancer Immunol. Res. 6 (8) (2018) 882–887.
[11] R.K. Selvaraj, Avian CD4(+)CD25(+) regulatory T cells: properties and therapeutic applications, Dev. Comp. Immunol. 41 (3) (2013) 397–402.
[12] A.M. Schmitt, H.Y. Chang, Long noncoding RNAs in cancer pathways, Cancer Cell 29 (4) (2016) 452–463.

[13] M.A. Parasramka, S. Maji, A. Matsuda, I.K. Yan, T. Patel, Long non-coding RNAs as novel targets for therapy in hepatocellular carcinoma, Pharmacol. Ther. 161 (2016) 67–78.
[14] L.J. Lim, S.Y.S. Wong, F. Huang, S. Lim, S.S. Chong, L.L. Ooi, et al., Roles and regulation of long noncoding RNAs in hepatocellular carcinoma, Cancer Res. 79 (20) (2019) 5131–5139.
[15] H. Ling, M. Fabbri, G.A. Calin, MicroRNAs and other non-coding RNAs as targets for anticancer drug development, Nat. Rev. Drug Discov. 12 (11) (2013) 847–865.
[16] Y. Du, G. Kong, X. You, S. Zhang, T. Zhang, Y. Gao, L. Ye, et al., Elevation of highly up-regulated in liver cancer (HULC) by hepatitis B virus X protein promotes hepatoma cell proliferation via down-regulating p18, J. Biol. Chem. 287 (31) (2012) 26302–26311.
[17] S. Dhamija, S. Diederichs, From junk to master regulators of invasion: lncRNA functions in migration, EMT and metastasis, Int. J. Cancer 139 (2) (2016) 269–280.
[18] S.H. Park, N.S. Veerapu, E.C. Shin, A. Biancotto, J.P. McCoy, S. Capone, et al., Subinfectious hepatitis C virus exposures suppress T cell responses against subsequent acute infection, Nat. Med. 19 (12) (2013) 1638–1642.
[19] P. Lapierre, A. Lamarre, Regulatory T Cells in autoimmune and viral chronic hepatitis, J Immunol Res 2015 (2015) 479703.
[20] R. Elling, J. Chan, K.A. Fitzgerald, Emerging role of long noncoding RNAs as regulators of innate immune cell development and inflammatory gene expression, Eur. J. Immunol. 46 (3) (2016) 504–512.
[21] J.H. Cha, L.C. Chan, C.W. Li, J.L. Hsu, M.C. Hung, Mechanisms controlling PD-L1 expression in cancer, Mol. Cell. 76 (3) (2019) 359–370.
[22] J. Zhao, Y. Fan, K. Wang, X. Ni, J. Gu, H. Lu, et al., LncRNA HULC affects the differentiation of Treg in HBV-related liver cirrhosis, Int. Immunopharm. 28 (2) (2015) 901–905.
[23] National Research Council (US), Committee for the update of the guide for the Care and use of laboratory animals, in: Guide for the Care and Use of Laboratory Animals, eighth ed., National Academies Press (US), 2011.
[24] C. Zhao, X. Wu, J. Chen, G. Qian, The therapeutic effect of IL-21 combined with IFN-γinducing CD4+CXCR5+CD57+T cells differentiation on hepatocellular carcinoma, J. Adv. Res. 36 (2022) 89–99.
[25] N. Percie du Sert, V. Hurst, A. Ahluwalia, S. Alam, M.T. Avey, M. Baker, et al., The ARRIVE guidelines 2.0: updated guidelines for reporting animal research, Br. J. Pharmacol. 177 (16) (2020) 3617–3624.
[26] C. Yang, C. Shangguan, C. Cai, J. Xu, X. Qian, LncRNA HCP5 participates in the Tregs functions in allergic rhinitis and drives airway mucosal inflammatory response in the nasal epithelial cells, Inflammation 45 (3) (2022) 1281–1297.
[27] R. Jiang, J. Tang, Y. Chen, L. Deng, J. Ji, Y. Xie, et al., The long noncoding RNA lnc-EGFR stimulates T-regulatory cells differentiation thus promoting hepatocellular carcinoma immune evasion, Nat. Commun. 8 (2017) 15129.
[28] H.D. Ochs, M. Oukka, T.R. Torgerson, TH17 cells and regulatory T cells in primary immunodeficiency diseases, J. Allergy Clin. Immunol. 123 (5) (2009) 977–983.
[29] L. Chen, L. Zheng, W. He, M. Qiu, L. Gao, J. Liu, et al., Cotransfection with IL-10 and TGF-β1 into immature dendritic cells enhances immune tolerance in a rat liver transplantation model, Am. J. Physiol. Gastrointest. Liver Physiol. 306 (7) (2014) G575–G581.
[30] Y. Fang, M.J. Fullwood, Roles, functions, and mechanisms of long non-coding RNAs in cancer, Dev. Reprod. Biol. 14 (1) (2016) 42–54.
[31] X. Tu, Y. Zhang, X. Zheng, J. Deng, H. Li, Z. Kang, et al., TGF-β induced hepatocyte lincRNA-p21 contributes to liver fibrosis in mice, Sci. Rep. 7 (1) (2017) 2957.
[32] S. Kumagai, S. Koyama, K. Itahashi, T. Tanegashima, Y.T. Lin, Y. Togashi, et al., Lactic acid promotes PD-1 expression in regulatory T cells in highly glycolytic tumor microenvironments, Cancer Cell 40 (2) (2022) 201–218.e9.
[33] Y. Li, Y. Li, S. Huang, Y. Li, Y. Li, S. Huang, K. He, M. Zhao, H. Lin, et al., Long non-coding RNA growth arrest specific transcript 5 acts as a tumour suppressor in colorectal cancer by inhibiting interleukin-10 and vascular endothelial growth factor expression, Oncotarget 8 (8) (2017) 13690–13702.
[34] M. Xie, J. Wei, J. Xu, Inducers, attractors and modulators of CD4+ Treg cells in non-small-cell lung cancer, Front. Immunol. 11 (2020) 676.
[35] D.H. Munn, M.D. Sharma, T.S. Johnson, Treg destabilization and reprogramming: implications for cancer immunotherapy, Cancer Res. 78 (18) (2018) 5191–5199.
[36] B.G. Wang, Z. Lv, H.X. Ding, X.X. Fang, J. Wen, Q. Xu, et al., The association of lncRNA-HULC polymorphisms with hepatocellular cancer risk and prognosis, Gene 670 (2018) 148–154.
[37] T.C. Tseng, C.J. Liu, H.C. Yang, T.H. Su, C.C. Wang, C.L. Chen, et al., High levels of hepatitis B surface antigen increase risk of hepatocellular carcinoma in patients with low HBV load, Gastroenterology 142 (5) (2012) 1140–1149.
[38] Y. Han, D. Liu, L. Li, PD-1/PD-L1 pathway: current researches in cancer, Am. J. Cancer Res. 10 (3) (2020) 727–742.
[39] T. Kamada, Y. Togashi, C. Tay, D. Ha, A. Sasaki, Y. Nakamura, et al., PD-1+ regulatory T cells amplified by PD-1 blockade promote hyperprogression of cancer, Proc Natl Acad Sci U S A. 116 (20) (2019) 9999–10008.
[40] Y. Zhuang, C. Liu, J. Liu, G. Li, Resistance mechanism of PD-1/PD-L1 blockade in the cancer-immunity cycle, OncoTargets Ther. 13 (2020) 83–94.
[41] X. Wang, Q. Dong, Q. Li, Y. Li, D. Zhao, J. Sun, et al., Dysregulated response of follicular helper T cells to hepatitis B surface antigen promotes HBV persistence in mice and associates with outcomes of patients, Gastroenterology 154 (8) (2018) 2222–2236.
[42] S. Kalathil, A.A. Lugade, A. Miller, R. Iyer, Y. Thanavala, Higher frequencies of GARP(+)CTLA-4(+)Foxp3(+) T regulatory cells and myeloid-derived suppressor cells in hepatocellular carcinoma patients are associated with impaired T-cell functionality, Cancer Res. 73 (8) (2013) 2435–2444.
[43] J. Li, X. Wang, J. Tang, R. Jiang, W. Zhang, J. Ji, et al., HULC and linc00152 act as novel biomarkers in predicting diagnosis of hepatocellular carcinoma, Cell. Physiol. Biochem. 37 (2) (2015) 687–696.
[44] Y. Ding, C. Sun, J. Li, L. Hu, M. Li, J. Liu, et al., The significance of long non-coding RNA HULC in predicting prognosis and metastasis of cancers: a meta-analysis, Pathol. Oncol. Res. 25 (1) (2019) 311–318.
[45] S. Hibino, S. Chikuma, T. Kondo, M. Ito, H. Nakatsukasa, S. Omata-Mise, et al., Inhibition of Nr4a receptors enhances antitumor immunity by breaking Treg-mediated immune tolerance, Cancer Res. 78 (11) (2018) 3027–3040.
[46] Y. Ohue, H. Nishikawa, Regulatory T (Treg) cells in cancer: can Treg cells be a new therapeutic target? Cancer Sci. 110 (7) (2019) 2080–2089.
[47] Pilato M. Di, E.Y. Kim, B.L. Cadilha, J.N. Prüßmann, M.N. Nasrallah, D. Seruggia, et al., Targeting the CBM complex causes Treg cells to prime tumours for immune checkpoint therapy, Nature 570 (7759) (2019) 112–116.
[48] L. Li, X. Liu, K.L. Sanders, J.L. Edwards, J. Ye, F. Si, et al., TLR8-mediated metabolic control of human Treg function: a mechanistic target for cancer immunotherapy, Cell Metabol. 29 (1) (2019) 103–123.
[49] P. Kumar, S. Saini, B.S. Prabhakar, Cancer immunotherapy with check point inhibitor can cause autoimmune adverse events due to loss of Treg homeostasis, Semin. Cancer Biol. 64 (2020) 29–35.
[50] X. Pei, X. Wang, H. Li, LncRNA SNHG1 regulates the differentiation of Treg cells and affects the immune escape of breast cancer via regulating miR-448/IDO, Int. J. Biol. Macromol. 118 (2018) 24–30.
[51] Z. Yu, H. Zhao, X. Feng, H. Li, C. Qiu, X. Yi, et al., Long non-coding RNA FENDRR acts as a miR-423-5p sponge to suppress the Treg-mediated immune escape of hepatocellular carcinoma cells, Mol. Ther. Nucleic Acids 17 (2019) 516–529.
[52] J. Zhao, Y. Fan, K. Wang, X. Ni, J. Gu, H. Lu, et al., LncRNA HULC affects thedifferentiation of Treg in HBV-related liver cirrhosis, Int. Immunopharm. 28 (2) (2015) 901–905.